Modeling of Surface Blowing as an Anti-icing Technique for Aircraft Surfaces

A.H. Tabrizi*
Indiana Institute of Technology, Fort Wayne, Indiana
and
E.G. Keshock†
University of Tennessee, Knoxville, Tennessee

An analysis of a proposed possible anti-icing technique applicable to aircraft surfaces has been studied and is described herein. Air injection at the leading edge of an ice-accreting surface is used to reduce and/or eliminate ice collection by preventing the supercooled water droplets in the atmosphere from impinging on the surface. In this envisioned technique, a discrete stream of fluid (air) is injected into the mainstream through slots located on the cylinder surface. The modified flow around the surface produces modified droplet trajectories, deflecting the droplets away from the surface. Exact mathematical expressions for the velocities are obtained from potential flow theory. Droplet trajectories are obtained for a variety of surface blowing conditions. It was found that for a given cylinder diameter, freestream velocity, droplet size, and injection, there is an optimum slot location for which the injection has its maximum effect, i.e., minimum water collection and subsequent ice accretion. The effect of injection rate as well as the number of slots on the collection efficiency are also investigated.

Nomenclature

a = acceleration
C_d = droplet drag coefficient
D = cylinder diameter
d = droplet diameter
E = collection efficiency
$\bar{F}$ = force vector
$\bar{F}_d$ = drag force vector
$\bar{F}_g$ = gravity force vector
Fr = Froude number
$g,\bar{g}$ = gravitational constant and vector
K = inertia parameter
LWC = liquid water content
m = mass
m_d = droplet mass
m_{ice} = accreted ice mass
Q = nondimensional slot (source) flow rate
q = slot flow rate or source/sink strength
R = cylinder radius
Re_d = droplet relative Reynolds number, $d(|U_a - U_d|)/\nu$
Re_{0d} = flow Reynolds number, dU_∞/ν
Re_0 = flow Reynolds number, RU_∞/ν
r = radial coordinate
r_d = droplet radius
$\bar{S}$ = droplet position vector
$\bar{S}^*$ = droplet position vector (nondimensional)
$\ddot{\bar{S}}^*$ = droplet acceleration vector (nondimensional)
t = time and duration of icing
$\bar{U}_a, \bar{U}_d$ = local air and droplet velocity vector, respectively
U_∞ = freestream velocity
u_a, u_d = air and droplet velocity in the x direction, respectively
v_a, v_d = air and droplet velocity in the y direction, respectively
x,y = Cartesian coordinates
x_d, y_d = droplet position in the x and y direction
x_i, y_i = position of a slot (source) on the cylinder
α,β,θ = angles defined in Fig. 3
μ = air viscosity
ν = air kinematic viscosity
ρ_d = droplet density
ρ_i = radial coordinate defined by Eq. (15)
ϕ = potential function and parameter defined by Re_{0d}^2/K
ψ = stream function

Presented as Paper 87-0026 at the AIAA 25th Aerospace Sciences Meeting, Reno, NV, Jan. 12–15, 1987; received March 23, 1987; revision received June 18, 1987.

*Assistant Professor, Department of Engineering. Member AIAA.
†Professor, Department of Mechanical Engineering. Member AIAA.

Introduction

PROBLEMS associated with aircraft icing have been recognized since the early days of aircraft technology and have been subject to a number of investigations. The undesirable effects of icing on aircraft performance and potential hazards associated with these effects have been well documented.

Icing occurs when an aircraft enters an atmosphere containing supercooled water droplets. Under such conditions, when a supercooled water droplet strikes the aircraft, a fraction of the droplet may freeze; the ice formed immediately adheres to the surface. Ice accreted on the wing surface increases the aerodynamic drag coefficient and decreases the lift. In the case of icing of a helicopter rotor blade, the blade drag is increased, resulting in a torque rise on the rotor shaft.[1]

Ice accretion process on a circular cylinder in droplet-ice crystal clouds is modeled by Lozowski et al.[2] and collection efficiencies and resulting ice shapes for different icing processes are predicted. Water drop trajectories about arbitrary three-dimensional bodies in potential flow is calculated by Norment.[3] He used the method developed by Hess and Smith to model the potential flowfield. Maltezos et al.[4] are in the process of developing a computer program to calculate particle trajectories for icing analysis of axisymmetric bodies.

Ice protection techniques can be categorized as anti-icing (the prevention of ice formation) and deicing (the periodic removal of ice already formed). Examples of anti-icing techniques are the chemical and coating processes used to prevent ice from adhering. Continuous heating of the surface was considered by Nichols.[5] He investigated the heat flux re-

quirements to provide an ice-free leading edge of the engine inlet for cruise missiles with a strip heater configuration. A glycol-exuding porous leading-edge ice protection system has been experimentally investigated by the NASA Lewis Research Center and British aircraft industries.[6] This system can be operated in a deicing mode as well as an anti-icing mode. Another deicing system includes pneumatic deicers ("rubber shoes" that cover the leading edge and are periodically inflated and deflated). Intermittent heating of airfoils utilizing hot air is considered by Hauger.[7]

In the present paper, an analysis is presented of another anti-icing technique, in which anti-icing is achieved by surface blowing of air counter to the mainstream. The injected air modifies the icing surface, i.e., displaces the streamlines about the surface, thus altering the droplet trajectories. The trajectories are elevated, resulting in reduction in the droplet collection efficiency of the surface. The extent of reduction of the collection efficiency is dependent on the blowing rate and other injection characteristics to be discussed later.

Analysis

In the following analysis, the icing surface, i.e., the leading edge of a wing or inlet of an engine, is approximated by a circular cylinder, with air injection taking place through a number of slots located along the frontal surface. The blowing at the surface displaces the streamlines at the surface, thus influencing the dynamics, i.e., trajectories, of the droplets in the atmosphere approaching the surface. Thus, to investigate the effect of surface injection on the ice collection rate (water collection rate), the determination of the modified droplet trajectories are required. Due to the presence of a droplet size spectrum in an atmospheric icing environment, it is advantageous to assume that the median volume diameter of droplets can effectively represent the average effect of all of the droplet sizes present in the stream, although it should be noted that one can use certain statistical functions to represent the droplet distribution in the flowfield. Choosing the coordinate system to be fixed on the aircraft system, the air stream containing the droplets is assumed to be uniform, steady, and laminar; also, the water droplets are distributed uniformly in the air.

Under these conditions, the droplet trajectories, in general, will be affected by the following factors and forces: two-phase flow effects, pressure gradient force, magnus lift force, Saffman lift force, temperature gradient effects, Basset memory force, droplet asphericity and breakup effects, electrostatic forces, apparent or virtual mass force, gravity force, and drag force. It can be shown that not all of these items are important in typical icing conditions.[8] Due to the small droplet loading (droplet mass/air mass), the two-phase flow effects are negligible, thus making it possible to obtain the solution of the flowfield independent of the droplets. Further analysis of the above items indicates that only the last two forces, namely, gravity and drag forces, are of significance in an icing situation.[8] The fact that the droplet loading in an icing environment is small ($\ll 0.1$) allows one to consider the droplet phase to be dilute,[9] i.e., not a continuum, thus making it possible to consider the motion of an individual droplet. The equation governing droplet dynamics is obtained by applying Newton's second law, $\bar{F}=m\bar{a}$, as

$$m_d \frac{d^2\bar{S}}{dt^2} = \bar{F}_g + \bar{F}_d \tag{1}$$

After inclusion of appropriate expressions and nondimensionalizing S, U, and t by R, U_∞, and R/U_∞, respectively (see Fig. 1 for the details of the coordinate system used), the nondimensional droplet trajectory equation is obtained as

$$\ddot{\bar{S}}^* = \frac{1}{Fr^2}\frac{\bar{g}}{g} - \frac{c_d Re_d}{24K}(\dot{\bar{S}}^* - \bar{U}_a) \tag{2}$$

where

$$K = \frac{\rho_d d^2 U_\infty}{9D\mu}, \qquad Fr = \frac{U_\infty}{(Rg)^{1/2}} \tag{3}$$

with the initial condition

$$t=0 \qquad u_d(x=10) = u_a \qquad v_d(x=10) = v_a \tag{4}$$

The nondimensional parameter K, commonly known as the inertia parameter, is the ratio of the aerodynamic response time to the residence time of the droplets. A droplet with a large aerodynamic response time compared to its residence time will be unable to react fast enough to the changes in the flow velocities; therefore, it will be separated from the streamlines and, depending on its trajectory, it can impact on the cylinder. Thus, one expects that the collection rate of the droplets on the cylinder to be higher for larger values of K. Equation (2) can now be integrated in the x and y direction to obtain the droplet trajectories. However, this equation requires knowledge of the local air velocity $\bar{U}_a$, which should be known at the droplet location. This vector velocity (for flow over a circular cylinder with surface blowing) is obtained from the analytical expressions derived herein. The use of these expressions is favored over a numerical computation scheme in which the velocities are computed at preselected grid points, the latter method required a series of interpolations for the velocities at the droplet location in a given cell. In addition, the computation time required by the analytical method used

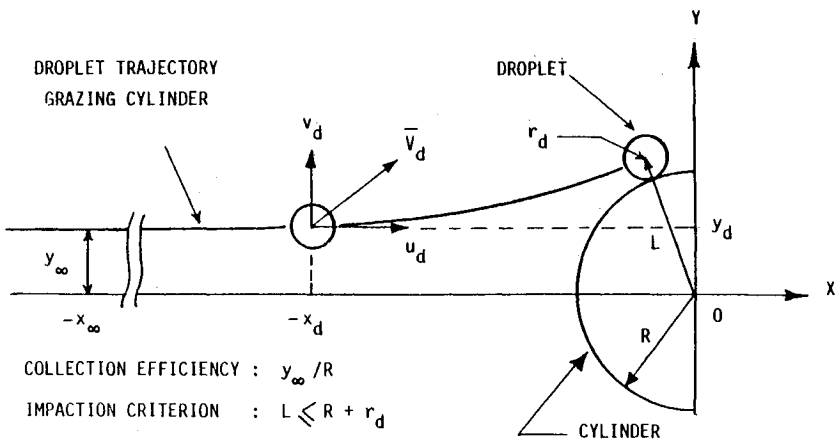

Fig. 1 Droplet coordinate system.

herein is several orders of magnitude smaller than that of the numerical method.

Theoretical Flow Model

A theoretical model is developed to calculate the velocities in the flow over a circular cylinder with surface injection. It is assumed that boundary-layer effects are negligible and that the entire flow can be represented by an inviscid flow. The freestream is assumed to be uniform and undisturbed by the presence of droplets. The entire flow is considered to be two-dimensional, with the cylinder represented by the superposition of a doublet within the uniform stream. Injection is considered to be taking place through the slots located at the frontal surface along the axis of the cylinder. The surface injection is modeled by representing the surface slots by line sources on the cylinder, which, in turn, requires the inclusion of line sinks at the center of the cylinder, as shown in Fig. 2. Specifically, for every source with a strength of q located on the cylinder, it is required to add a sink with the strength of $q/2$ at the center of the cylinder (circle). The requirement for the addition of sinks will be evident if one considers the image of a source outside a curved surface and the application of the circle theorem.[10,11] Both the stream and potential functions for the entire flow can now be obtained directly by summing up the stream, doublet, sources, and sinks. Thus,

$$\psi = \psi_{\substack{\text{uniform}\\\text{stream}}} + \psi_{\text{doublet}} + \sum_{i=1}^{n} \psi_{i_{\text{source}}} + \sum_{i=1}^{n} \psi_{i_{\text{sink}}} \tag{5}$$

$$\phi = \phi_{\substack{\text{uniform}\\\text{stream}}} + \phi_{\text{doublet}} + \sum_{i=1}^{n} \phi_{i_{\text{source}}} + \sum_{i=1}^{n} \phi_{i_{\text{sink}}} \tag{6}$$

Substituting appropriate stream and potential functions, Eqs. (5) and (6) become (coordinate details are given in Fig. 3)

$$\psi = U_\infty y - \frac{R^2 U_\infty y}{(x^2+y^2)} + \sum_{i=1}^{n} \frac{(q_i)(\theta_{\text{source}})_i}{2\pi} - \sum_{i=1}^{n} \frac{(q_i)(\theta_{\text{sink}})_i}{4\pi} \tag{7}$$

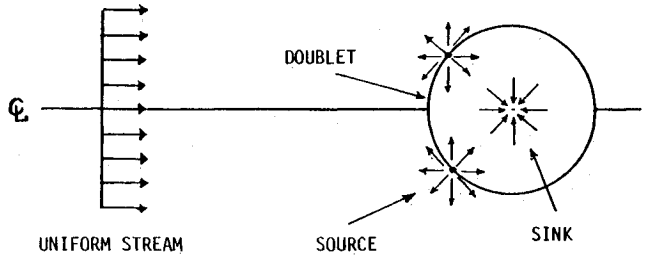

Fig. 2 Potential flow representation of flow over cylinder with surface injection.

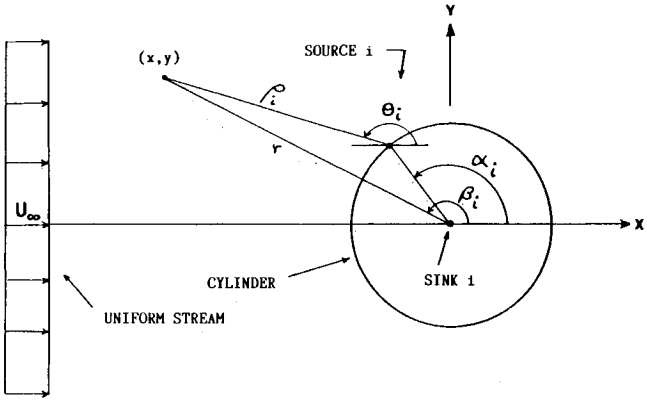

Fig. 3 Coordinate system of theoretical model.

where

$$(\theta_{\text{source}})_i = \tan^{-1}\frac{y-y_i}{x-x_i} \tag{8}$$

$$(\theta_{\text{sink}})_i = \tan^{-1}\frac{y}{x} \tag{9}$$

$$x_i = R\cos(\alpha_i) \tag{10}$$

$$y_i = R\sin(\alpha_i) \tag{11}$$

$$x = r\cos(\beta_i) \tag{12}$$

$$y = r\sin(\beta_i) \tag{13}$$

$$\phi = U_\infty x + \frac{R^2 U_\infty x}{(x^2+y^2)} + \sum_{i=1}^{n} \frac{q_i}{2\pi} \ln\rho - \sum_{i=1}^{n} \frac{q_i}{4\pi} \ln r \tag{14}$$

where

$$\rho = |(x-x_i)^2 + (y-y_i)^2|^{1/2} \tag{15}$$

$$r = |x^2+y^2|^{1/2} \tag{16}$$

The velocities were obtained from

$$u_a = \frac{\partial\phi}{\partial x} \tag{17}$$

$$u_a = U_\infty \left|1 - \frac{R^2(x^2+y^2)}{(x^2+y^2)}\right|_{\substack{\text{uniform}\\\text{stream}}} + \sum_{i=1}^{n} \frac{q_i}{2\pi} \frac{(x-x_i)}{(x-x_i)^2+(y-y_i)^2} - n\sum_{i=1}^{n} \frac{q_i}{4\pi} \frac{x}{(x^2+y^2)} \tag{18}$$

Similarly,

$$v_a = +\frac{\partial\phi}{\partial y} \tag{19}$$

$$v_a = -\frac{2R^2 U_\infty xy}{(x^2+y^2)^2} + \sum_{i=1}^{n} \frac{q_i}{2\pi} \frac{y-y_i}{(x-x_i)^2+(y-y_i)^2} - n\sum_{i=1}^{n} \frac{q_i}{4\pi} \frac{y}{(x^2+y^2)} \tag{20}$$

The trajectory equation can now be integrated with the aid of the above air velocities. The integration process was terminated when the trajectory of a droplet, released from a distance $10R$ ahead of the cylinder, intercepted the cylinder or passed the cylinder. It was assumed that the droplet was collected on the cylinder when the impaction criterion was satisifed, i.e., $L \le R + r_d$, as shown in Fig. 1. It should be noted that the criterion used to evaluate the system performance is the parameter called "collection efficiency," which is represented by the symbol E. Figure 1 also graphically presents the definition of the collection efficiency. The effect of surface blowing on the ice collection is then judged by the reduction in the collection efficiency. The collection efficiency of the circular cylinder without surface blowing was first determined and plotted against the inertia parameter K as shown in Fig. 4. A dimensionless parameter ϕ, defined as

$$\phi = Re_{0d}^2/K \tag{21}$$

and used for the presentation of the data, is valuable in that it is not a function of droplet diameter; additionally its magnitude is a measure of the deviation from Stokes' law for the forces acting on the water droplets.[12]

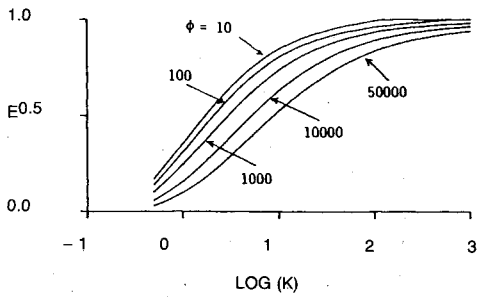

Fig. 4 Collection efficiency of cylinder.

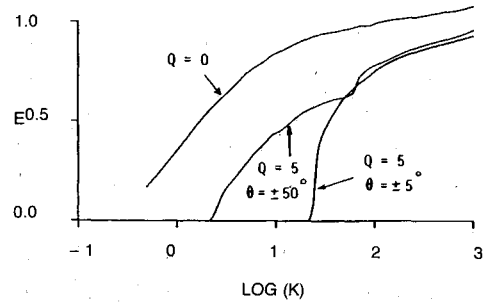

Fig. 5 Collection efficiency of cylinder with surface injection, sources located at ±5 and ±50 deg.

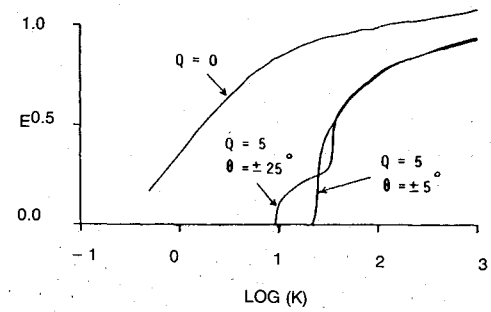

Fig. 6 Collection efficiency of cylinder with surface injection, sources located at ±5 and ±25 deg.

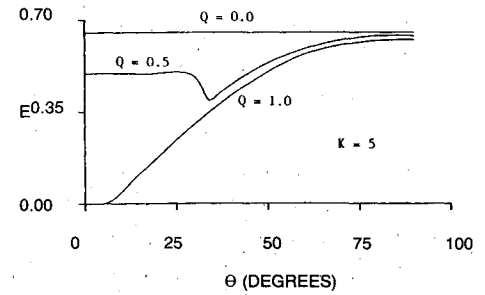

Fig. 7 Effect of source location on collection efficiency for two sources located at ±θ deg, $K=5$.

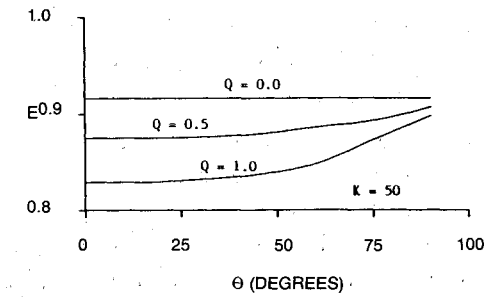

Fig. 8 Effect of source location on collection efficiency for two sources located at ±θ deg, $K=50$.

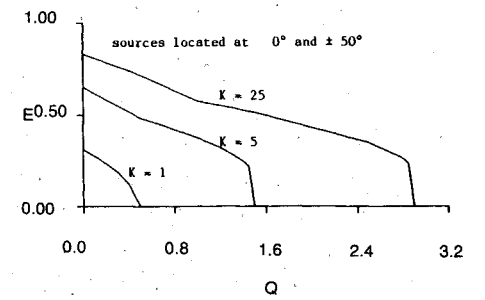

Fig. 9 Effect of source strength on collection efficiency, three source model.

It is reasonable that the collection of a circular cylinder with surface injection depends on the source (slot) location, source flow rate, and number of sources present on the cylinder. The collection efficiency of a circular cylinder, in which two sources are located at $\pm\theta$ deg from the front stagnation point (line), have been calculated and plotted in Fig. 5 for a value of the ϕ parameter of 10. For the two sources located at ±50 deg from the front stagnation point, with a source strength of $Q=5$, (Q is the nondimensional source strength, i.e., $Q=q/RU_\infty$), it is apparent that the collection efficiencies E have been reduced considerably compared to the case where there is no injection, i.e., where $Q=0$. (It will be shown later that as the source strength is increased the collection efficiencies are further reduced.) Figure 5 also presents another case where the sources are located at ±5 deg for $Q=5$. In this case, the reduction in the collection efficiency values are even greater.

Consider another case where the slots are located at ±25 and ±5 deg as shown in Fig. 6. Once again the reduction in the collection efficiency is evident. Examining the region where the two curves cross in both Figs. 5 and 6, one can anticipate that there should be an optimum location where the sources have their maximum effect on the collection efficiency. Thus, the next logical step of the analysis would be to find this particular location. Collection efficiencies have been plotted vs the source location (actually two sources, located at $\pm\theta$ deg for purpose of symmetry) and shown in Fig. 7. A general reduction in the collection efficiency compared to the case of no injection is realized. However, it can be seen that for the case shown there is an optimum source location at about $\theta=\pm34$ deg where the injection effect is a maximum, i.e., there is a maximum reduction in the collection efficiency, which is indicated by a dip on the curve.

Figure 6 indicates that the effect of injection diminishes as the sources move toward $\theta=\pm90$ deg. Figure 6 also contains a case with a higher source strength Q; the figure shows that the optimum location has been moved even further toward the front stagnation point, with further reduction in the collection efficiencies. The same analysis has been done with a larger value of K; the results are presented in Fig. 8. It is easily seen that in this case the location of the sources do not seem to have too much of an effect on the collection efficiency. This observation leads one to believe that, for the two slow models, there is only one optimum source location for a particular case for a given droplet diameter, cylinder diameter, and freestream velocity.

Dependence of the collection efficiency on the injection flow rate is shown in Fig. 9. This figure presents the case in which there are three injection slots (sources) on the cylinder, which are located at −50, 0, and +50 deg (where 0 deg corresponds to the front stagnation line). It can be seen that as the injection flow rates are increased the collection efficiency of the cylinder is decreased. Furthermore, the required injection rate for a 100% reduction in efficiency is greater for a larger inertia parameter K. This is obvious from physical grounds since a larger value of K implies either a large freestream velocity or a larger droplet size.

The effect of the number of injection slots on the collection efficiency was studied and results are shown in Fig. 10. The slots were considered to be equally spaced on the front half of

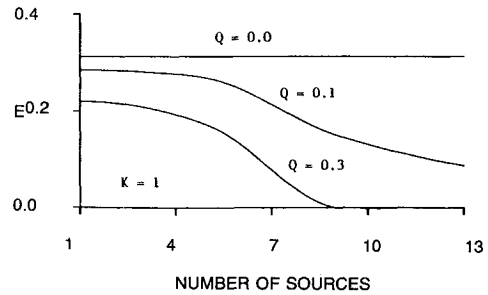

Fig. 10 Effect of source numbers on collection efficiency for equally spaced sources within ±90 deg.

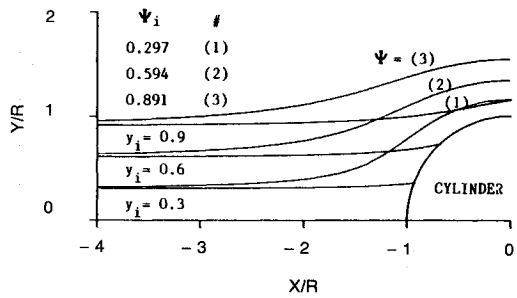

Fig. 11 Droplet trajectories and streamlines, $K=10$, $\phi=1000$, and $Q=0$.

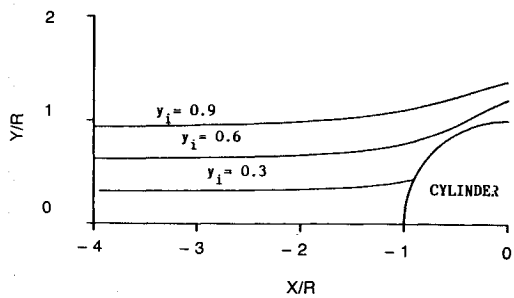

Fig. 12 Droplet trajectories, $K=10$, $\phi=1000$, $Q=0.5$, source angles 0, ±30, and ±60 deg.

the cylinder (i.e., from +90 to −90 deg, where angles are measured from the front stagnation line). For example, in the case of the three-slot model, the slots are located at the front stagnation point and at ±90 deg. As would be expected and as shown in Fig. 10, the collection efficiency decreases with an increase in the number of sources. However, it should be noted that the same reduction in efficiency can also be achieved by holding the source numbers constant and increasing the injection rate, as is also shown in this figure.

It should also be noted that there is an optimum number of sources for which there is no collection at all, i.e., $E=0$. It is shown in Fig. 10 that the minimum number of sources required to reduce efficiency to $E=0$ for the case of $K=1.0$ and injection rate of $Q=0.3$ is 9.

The trajectories of the droplets for the case of flow over a circular cylinder without any surface blowing are shown in Fig. 11. This figure also contains the corresponding streamlines at $x=-10R$ where the trajectories coincide with the streamlines. The separation of droplet trajectories from streamlines as the droplets approach the cylinder should next be established. Such effects of surface blowing on droplet trajectories are shown in Fig. 12. A total of five sources, located at 0, ±30, and ±60 deg from the front stagnation point, with a source flow of $Q=0.5$ were considered.

Finally, Fig. 13 presents a case of strong blowing for the same case discussed above. In this case, droplets are being repelled or blown away from the surface. The closest trajectory to the surface is most affected. The effect of various blowing rates on a particular trajectory is shown in Fig. 14. This figure presents three curves for three different values of source strength, i.e., $Q=0$, 1.0, and 2.0, for droplets initially released from $y=0.3$ and $x=10R$. The source numbers and

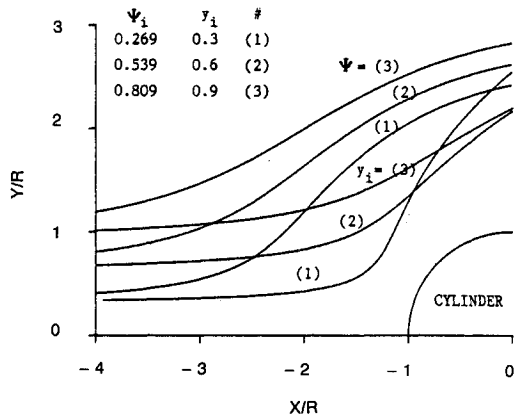

Fig. 13 Droplet trajectories and streamlines, $K=10$, $\phi=1000$, and $Q=2$, source angles 0, ±30, and ±60 deg.

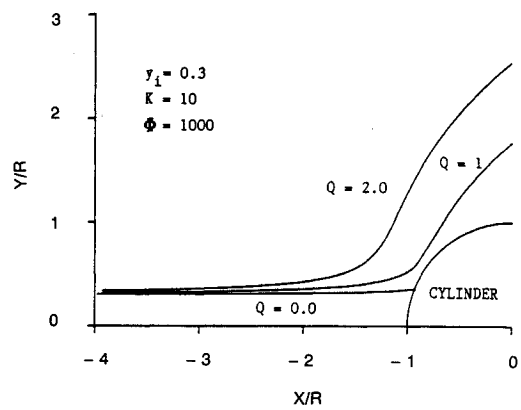

Fig. 14 Droplet trajectories for various source strengths.

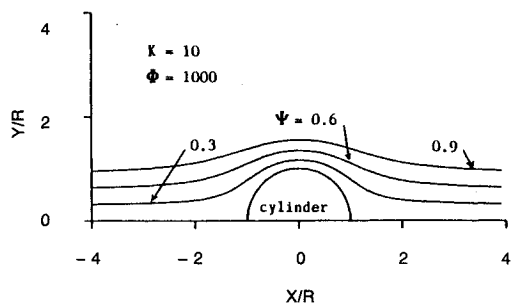

Fig. 15 Streamlines of flow over circular cylinder.

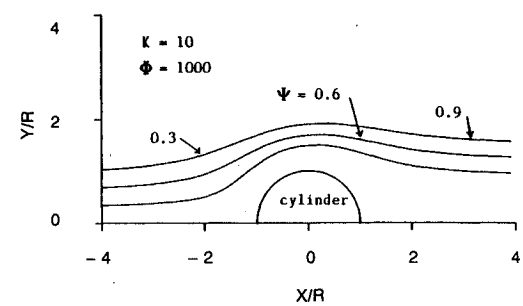

Fig. 16 Streamlines of flow over circular cylinder with surface injection $Q=0.5$, angles 0, ±30, and ±60 deg.

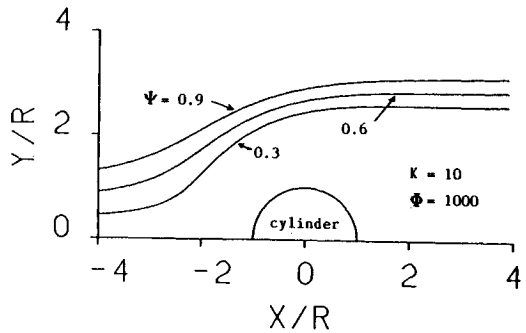

Fig. 17 Streamlines of flow over circular cylinder with surface injection $Q=2$, source angles 0, ± 30, and ± 60 deg.

their locations on the cylinder are the same as those discussed above. Figures 15–17 show the effect of surface blowing on the flow streamlines. Elevation of the streamlines ahead of and behind the cylinder is indicated. Once again, a total of five sources, located at 0, ± 30, and ± 60 deg from the stagnation point, were considered.

The amount of ice collection on the cylinder can now be calculated from

$$m_{\text{ICE}} = (E)\,(\text{LWC})\,(U_\infty)\,(D)\,(t) \tag{22}$$

The results that may be so obtained from the present analysis have been found to compare favorably to those obtained experimentally.[8] The results of the experimental investigation of ice formation on a cylinder with surface blowing will appear in a future publication.

Conclusions

The flow model analyzed herein appears to indicate that air injection through slots strategically located on the frontal surface of an airfoil can significantly influence the trajectories of incoming droplets, so as to reduce the amount of drops impinging on the surface. This therefore suggests a possible means of reducing ice accretion on aircraft surfaces. However, it should be noted that other effects of surface injection, e.g., the aerodynamic characteristics (i.e., lift, drag, etc.) of the icing surface, should also be investigated to further establish the feasibility of this technique.

The results of the analytical modeling technique (source and sink representation of the injection slots) presented herein have been found to compare well with the potential flow solution obtained numerically,[8] thus indicating the applicability of this simplified model to fairly complex problems.

References

[1]Lake, H.B. and Bradley, J., "The Problem of Certifying Helicopters for Flight in Icing Conditions," *Aeronautical Journal,* Vol. 80, 1976, pp. 419–433.

[2]Lozowski, E.P. et al., "The Icing of an Unheated Non-rotating Cylinder in Liquid Water Droplet-Ice Crystal Clouds," National Research Council of Canada, Rept. LTR-LT-96, 1979, p. 09.

[3]Norment, H.G., "Calculation of Water Drop Trajectories to and About Arbitrary Three-Dimensional Bodies in Potential Airflow," NASA, CR-3291, Aug. 1980.

[4]Maltezos, D.G. et al., "Particle Trajectory Computer Program for Icing Analysis of Axisymmetric Bodies (A Progress Report)," AIAA Paper 87-1215, Jan. 1987

[5]Nichols, C.C., "Ice Protection of Engine Air Inlet for Cruise Missile Applications," ASME Paper 80-ENAS-2, 1980.

[6]Kohlman, D.L. et al., "Icing Tunnel Tests of a Glycol-Exuding Porous Leading Edge Ice Protection System on a General Aviation Airfoil," AIAA Paper 81-0405, 1981.

[7]Hauger, H.H., "Intermittent Heating of Airfoils for Ice Protection, Utilizing Hot Air," ASME Paper 53-SA-42, March 1953.

[8]Tabrizi, A.H., "An Experimental and Theoretical Investigation of an Air Injection Type Anti-Icing System for Aircraft," Ph.D. Dissertation, University of Tennessee, Knoxville, 1986.

[9]Crowe, C.T., "Conservation Equations for Vapor-Droplet Flows Including Boundary-Droplet Effects," Lawrence Livermore Laboratory, Livermore, CA, Rept. UC-66, 1976.

[10]Milne-Thomson, L.M., *Theoretical Hydrodynamics,* 5th ed., Macmillan, New York, 1968.

[11]Lamb, S.H., *Hydrodynamics,* Dover Publications, New York, 1945.

[12]Brun, R.J. et al., "Impingement of Cloud Droplets on a Cylinder and Procedure for Measuring Liquid-Water Content and Droplet Sizes in Supercooled Clouds by Rotating Multicylinder Method," NACA TN-1215, 1955.